Studies in Surface Science and Catalysis 130
A. Corma, F.V. Melo, S.Mendioroz and J.L.G. Fierro (Editors)

Metal particles on oxide surfaces: structure and adsorption behaviour

M. Bäumer*, M. Frank, R. Kühnemuth, M. Heemeier, S. Stempel and H.-J. Freund

Fritz-Haber-Institut der Max-Planck-Gesellschaft, Faradayweg 4-6, 14195 Berlin, Germany

Although deposited metal particles play an important role as heterogeneous catalysts, there is only limited fundamental knowledge about the relationship between their structure, their adsorption behaviour and their catalytic activity. In this article, we describe a strategy giving access to suitable model systems which can be studied with most surface spectroscopic and microscopic techniques. These systems are based on thin oxide films as supports, onto which metal particles of controllable size are grown by vapour deposition. As concrete examples, the preparation of Ir, Pd and Rh aggregates as well as their interaction with CO and C_2H_4 will be discussed.

1. INTRODUCTION

Deposited metal particles play a central role in heterogeneous catalysis. Many catalysts consist of an active component, such as a transition metal, which is dispersed over a suitable support material - usually an oxide, such as alumina or silica. In the first place, this is done in order to achieve the highest possible surface area of the active phase. Because of the high degree of dispersion, however, particle size effects and metal substrate interactions can influence the catalytic behaviour significantly. Of course, it has always been an important question in catalytic research how these effects can be exploited to improve the activity or the selectivity of a supported catalyst [1]. Nevertheless, on a fundamental level, there is still only very limited knowledge about these relationships. In order to contribute to a better understanding, we have investigated a number of model systems based on thin, well-ordered oxide films [2,3]. From an experimental point of view, such supports have the advantage of good electrical and thermal conductivities as compared to oxide bulk materials. Hence, many powerful surface analytical tools, i.e. electron spectroscopies and scanning tunneling microscopy (STM), can be applied without charging problems [2-4].

The films can be either prepared by oxidation of a suitable metal substrate or by deposition of the corresponding element onto a host crystal followed by oxidation in an oxygen ambient [2-4]. An extremely well-ordered *alumina film*, for example, can be grown on a NiAl(110) surface [5], whereas a thin *silica film* is obtainable by the second technique using a Mo(112) support [6]. In the case of the alumina film which originally contains no hydroxyl groups, it has furthermore been possible to introduce OH groups by subsequent treatment with aluminium and water [7].

Onto the thin alumina film, we have vapour deposited a large number of metals including Ag, Pt, Pd, Rh, Ir, Co and Al [2]. After characterising their structure and morphology in detail with STM and electron diffraction, the adsorption and reaction behaviour has been studied using suitable probe molecules, such as CO and C_2H_4. In this article, we will focus on three examples, namely Pd, Rh and Ir, for which we will discuss the nucleation and growth behaviour under different preparation conditions first. These data show that it is possible to obtain a large spectrum

* Corresponding author. Fax: +49 30-8413-4312. *E-mail address*: baeumer@fhi-berlin.mpg.de

of different particle sizes and morphologies in a controlled state. The remaining part of the paper deals with adsorption experiments revealing interesting dependencies on cluster size and type of metal.

2. EXPERIMENTAL

The experiments were conducted in *ultrahigh vacuum systems*, equipped with STM instruments, photoemission and electron diffraction facilities and all instruments necessary for the preparation of the surface. The infrared spectra have been taken in situ with a Bruker vacuum IR spectrometer in reflection geometry. The ordered *Al_2O_3 film* was obtained as previously described in the literature, i.e. by oxidation of a NiAl(110) single crystal surface and subsequent annealing [2,5]. The *metals* (> 99.9 %) were evaporated with commercial evaporators based on electron bombardment. Their flux was calibrated by a quartz microbalance and checked via STM. The deposition rates varied between 0.1 - 0.6 ML min^{-1} (ML: monolayer). The sample temperature during deposition was either 90 K or 300 K.

3. THE SUPPORT: Al_2O_3/NiAl(110)

As already mentioned, the support for all systems discussed in this article is a thin alumina film which can easily be prepared on the (110) surface of a NiAl alloy single crystal. The most prominent feature of this film is its high degree of long-range order setting it apart from the amorphous alumina films grown on Al single crystals. Another advantage is the excellent reproducibility of its structure, thickness and defect density [2]. Without going into details, a few features should be mentioned here [2]:

- The thickness of the film is 5 Å, corresponding to two layers of oxygen (and aluminium).
- The oxide overlayer contains no Ni ions and is free of hydroxyl groups.
- According to the phonon spectrum, the film has a structure which is similar to γ-Al_2O_3.
- The oxygen ions form a quasi-hexagonal structure on the surface.
- The band gap (~ 8 eV) is in reasonable agreement with the bulk material.
- Most simple molecules, including CO, do not adsorb on the pristine film at and above 90 K.
- The film exhibits a characteristic defect structure which is dominated by a network of antiphase and reflection domain boundaries [5]. While the first type is the result of a lateral displacement between two adjacent oxide areas, the latter separates domains with two different azimuthal orientations (result of the twofold symmetry of the NiAl support). Apart from the line defects, a certain concentration (~10^{13} cm^{-2}) of point defects is present on the surface.

4. NUCLEATION AND GROWTH BEHAVIOUR OF Pd, Rh AND Ir

Figure 1 contains a series of STM images taken (at 300 K) after deposition of Pd, Rh and Ir onto the thin alumina film at 90 K and 300 K. Considering the 90 K deposits first, a relatively isotropic arrangement of particles on the surface is obtained in all cases. (Note that neither the domain boundaries, which are visible as protruding lines in the pictures, nor the steps play a dominant part). Since the particle densities found for these and various other metals are nearly the same, it can be concluded that all metals follow a common nucleation behaviour under these conditions. In order to gain more information on this question, experiments at different evaporation fluxes have been conducted [8]. They revealed that a homogeneous nucleation mechanism can be ruled out, i.e. the *point defects* of the film act as nucleation centres at 90 K.

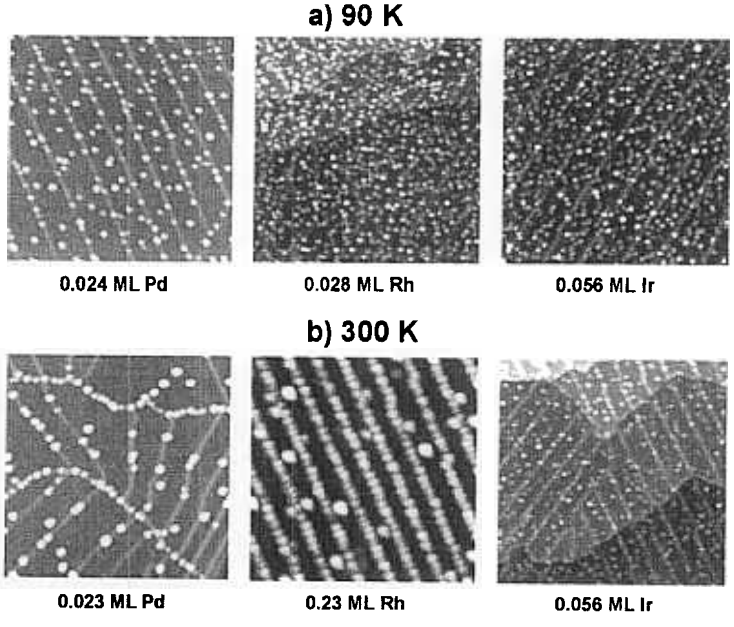

Fig. 1. Series of STM images (CCT, all pictures: 1000 × 1000 Å) taken after deposition of small amounts of Pd, Rh and Ir on the thin alumina film at (a) 90 K and (b) 300 K (data acquisition at 300 K).

Comparing the situation at 90 K with the one at 300 K, differences between the three metals can clearly be detected. Rh and Pd apparently prefer different nucleation sites now, while Ir largely reproduces its behaviour at 90 K. In the first case, an almost exclusive decoration of the domain boundaries, especially of the curved boundaries, and steps is observed. So, heterogeneous nucleation still governs the growth, but the *line defects* are the primary nucleation centres at 300 K. Evidently, they offer sites with a higher adsorption energy, which, however, only come into play if the thermal mobility is sufficient to reach them. An explanation for the deviating behaviour of Ir could simply be that it interacts less strongly with the line defects. More likely, though, is an increased metal support interaction resulting in a decreased mobility on the surface. This interpretation is in line with the higher oxygen affinity of Ir.

As shown in Fig. 2, a large spectrum of particle sizes can be prepared by taking advantage of different preparation conditions. At 90 K, very small clusters consisting of just a few atoms can be grown in the low coverage regime. At higher coverages, particles up to several hundred atoms are accessible as well. For Rh and Pd, somewhat larger aggregates may be obtained by switching to 300 K. In the case of Pd, a large number of these aggregates are even crystalline with clearly developed facets (mainly (111)) [2,9].

5. CO ADSORPTION

In Fig. 3, infrared spectra of Pd, Rh and Ir deposits of different size are presented which have been taken after CO saturation at 90 K. From the wealth of information which can be extracted from these data, only a few aspects should be referred to in this context.

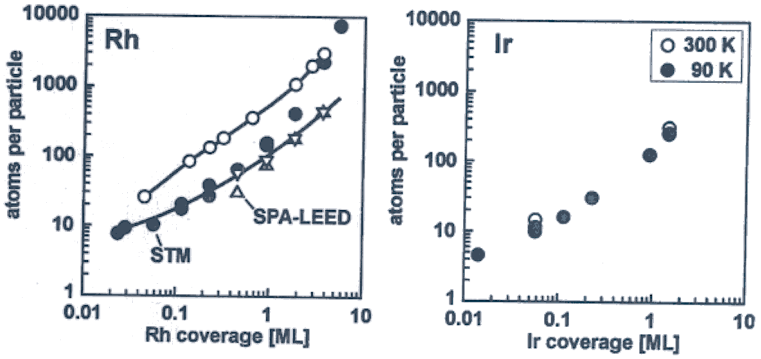

Fig. 2. Average number of atoms per particle for Rh (left) and Ir (right) deposits as determined by STM and SPA-LEED (profile analysis of LEED spots [2]). Full (open) circles: deposition at 90 K (300 K).

In the regime of very low coverages (Fig. 3 (a)), several sharp bands can be discerned in the case of Rh and Ir clearly pointing to the formation of small, well-defined carbonyl species upon CO adsorption. The signal at 2117 cm^{-1} in the Rh spectrum, for instance, has been assigned to a $Rh(CO)_2$ species resulting from single Rh atoms trapped at the point defects of the support [10]. For Ir, the corresponding absorption peak can be found at 2107 cm^{-1}, but, as deduced from the other sharp bands at lower wavenumbers, other types of carbonyls exist here as well. Pd, on the other hand, neither seems to form a dicarbonyl nor other distinct carbonyl species. Of course, the question arises whether the Rh and Ir species develop during CO adsorption (due to the disruption of larger particles, e.g. [11]) or originate from aggregates already existing. In fact, the first alternative has been excluded by annealing experiments ensuring that the experiments probe the original particle ensemble [10].

Turning to larger particles, broader bands can be detected which are due to CO adsorbed on bridge/hollow sites (Pd: < 2020 cm^{-1}, Rh: < 1970 cm^{-1}, Ir: not detectable) and on-top sites. Considering all three sets of spectra in Fig. 3, it turns out that the portion of the first species decreases in the series Pd > Rh > Ir, in agreement with measurements on single crystals. For Pd, it is furthermore obvious that the portion of terminally bonded CO increases as the particle size decreases ((a) → (c)). This change is also accompanied by a weakening of the Pd-CO bond, as deduced from photoelectron spectroscopic measurements [2,12].

Not surprisingly, the best ordered particles are obtained at 300 K. Here, the bands are clearly sharper than at 90 K. Especially, note the difference in the regime of terminally bonded CO for Ir ıd Rh. Only for the 90 K deposits, a shoulder signal at 2050 cm^{-1} appears. Since such a feature can be attributed to defect sites, i.e. kinks and steps [10], the data prove that the particles grown at 90 K exhibit a much higher defect density than the 300 K deposits. As mentioned, the Pd particles grown at 300 K are even crystalline. In fact, the corresponding bands can be assigned to specific facets on the aggregates [13]. The signals at 2108, 1956 and 1892 cm^{-1} are, for example, due to CO on (111) facets, whereas the peak at 2002 cm^{-1} is likely to be caused by CO on (100) facets ıd CO adsorbed on edge sites.

Summing up, the results demonstrate on the one hand that IR spectroscopy with a suitable probe molecule can be a powerful tool to trace particle morphologies. On the other hand, they reveal interesting dependencies of the CO adsorption site on particle size and the position of the ɛtal in the periodic table.

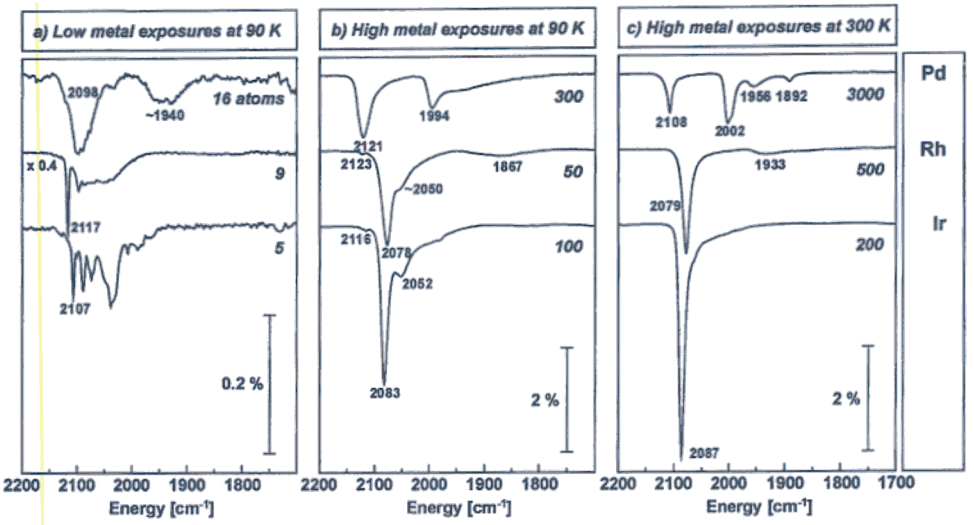

Fig. 3. IR spectra of Ir, Rh and Pd particles of different size and order saturated with CO at 90 K (data acquisition at 90 K). Average particle sizes are given next to the spectra.

6. C_2H_4 ADSORPTION AND REACTIVITY

Molecularly adsorbed C_2H_4 may be present on transition metal surfaces in two forms [14]. A weakly bound species, which is thought to be the primary intermediate in ethylene hydrogenation, is usually referred to as π-bonded ethylene. It is only weakly perturbed upon adsorption. The formation of the second type, di-σ-bonded ethylene, involves a stronger rehybridisation of the carbon atoms, increasing their sp^3 character. Upon heating, it dehydrogenates to ethylidyne, C_2H_3. Both, di-σ-bonded ethylene and ethylidyne are regarded as spectator species in the hydrogenation reaction. Ethylene rehybridisation upon adsorption results in a downshift of the strongly coupled C-C stretching and CH_2 scissoring modes from their gas phase frequencies of 1623 and 1342 cm^{-1}. As a semiquantitative measure of this perturbation, a πσ parameter has been proposed [15], defined by πσ = [(1623-band I)/1623) + (1342-band II)/1342] / 0.366. Here, 'band I' refers to the higher and 'band II' to the lower frequency of the C-C stretch - CH_2 scissors coupled pair. A higher πσ parameter indicates a larger extent of ethylene rehybridisation.

Upon saturation of Pd, Rh, and Ir particles containing about 200 metal atoms with C_2H_4 at 90 K, features typical for π-bonded ethylene are observed in the infrared spectra (Fig. 4). Signatures of molecules in the di-σ state are not so readily discerned. In the case of Pd, however, a weak band at ~1115 cm^{-1} and a C-H stretch signal at 2924 cm^{-1} may point to the presence of such species [16]. A comparatively high proportion of π-bonded ethylene may be due to the abundance of step and defect sites on small metal particles. Such sites have been suggested to favour the formation of the π-bonded form [17].

From the observed trend in vibrational frequencies, which decrease according to the sequence Pd > Rh > Ir, we may infer that the interaction of π-bonded ethylene with the metals increases from Pd across Rh to Ir. Making use of the πσ parameter to quantify these observations, we obtain values of 0.40 for Pd, 0.48 for Rh and approximately 0.55 for Ir. These findings agree well with results obtained on π-bonded ethylene on Me/Al_2O_3 catalysts [16,18]. This indicates that the

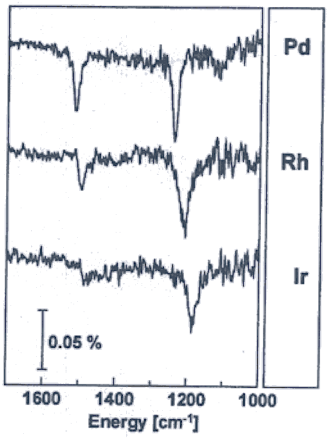

Fig. 4. IR spectra of Ir, Rh and Pd particles (size: ~ 200 atoms) saturated with C_2H_4 at 90 K (data acquisition at 90 K)

model systems are well suited for more extensive studies on hydrocarbon reactivity which are currently under way.

ACKNOWLEDGEMENTS

We are grateful to a number of agencies for financial support: Deutsche Forschungsgemeinschaft, Bundesministerium für Bildung und Forschung, Fonds der Chemischen Industrie and NEDO International Joint Research Grant on Photon and Electron Controlled Surface Processes. This work has also been supported, in part, by Synetix, a member of the ICI group, through their Strategic Research Fund. M.F. thanks the Studienstiftung des deutschen Volkes for a fellowship.

REFERENCES

1. M. Che, C.O. Bennett, Adv. Catal. 20 (1989) 153.
2. M. Bäumer, H.-J. Freund, Prog. Surf. Sci. 61 (1999) 127.
3. H.-J. Freund, Angew. Chem. Int. Ed. Engl. 36 (1997) 452.
4. D.W. Goodman, Surf. Rev. Lett. 2 (1995) 9; Surf. Sci. 299/300 (1994) 837.
5. J. Libuda, F. Winkelmann, M. Bäumer, H.-J. Freund, Th. Bertrams, H. Neddermeyer, K. Müller, Surf. Sci. 318 (1994) 61.
6. Th. Schröder, M. Adelt, M. Naschitzki, M. Bäumer, H.-J. Freund, in preparation.
7. J. Libuda, M. Frank, A. Sandell, S. Andersson, P.A. Brühwiler, M. Bäumer, N. Mårtensson , H.-J. Freund, Surf. Sci. 384 (1997) 106.
8. M. Bäumer, M. Frank, M. Heemeier, R. Kühnemuth, S. Stempel, H.-J. Freund, submitted to Surf. Sci.
9. K.H. Hansen, T. Worren, S. Stempel, E. Lægsgaard, M. Bäumer, H.-J. Freund, F. Besenbacher, I. Stensgaard, submitted to Phys. Rev. Lett..
10. M. Frank, R. Kühnemuth, M. Bäumer, H.-J. Freund, Surf. Sci. 427-428 (1999) 288; submitted to Surf. Sci.
11. F. Solymosi and M. Pásztor, J. Phys. Chem 89 (1985) 4789.
12. A. Sandell, J. Libuda, P.A. Brühwiler, S. Andersson, M. Bäumer, A.J. Maxwell, N. Mårtensson, H.-J. Freund, Phys. Rev. B. 55 (1997) 7233.
13. K. Wolter, O. Seiferth, H. Kuhlenbeck, M. Bäumer, H.-J. Freund, Surf. Sci. 399 (1998) 190.
14. P.S. Cremer, G.A. Somorjai, J. Chem. Soc. Faraday Trans. 91 (1995) 3671.
15. E.M. Stuve, R.J. Madix, C.R. Brundle, Surf. Sci. 152/153 (1985) 532.
16. S.B. Mohsin, M. Trenary, H.J. Robota, J. Phys. Chem. 95 (1991) 6657.
17. P.A. Dilara, W.T. Petrie, J.M. Vohs, Appl. Surf. Sci. 115 (1997) 243.
18. Y. Soma, J. Catal. 59 (1979) 239.